

Indium–gallium–zinc–oxide layer used to increase light transmittance efficiency of adhesive layer for stacked-type multijunction solar cells

Shinya Yoshidomi, Shunsuke Kimura, Masahiko Hasumi, and Toshiyuki Sameshima*

Tokyo University of Agriculture and Technology, Koganei, Tokyo 184-8588, Japan
 E-mail: tsamesim@cc.tuat.ac.jp

Received April 12, 2015; accepted July 30, 2015; published online October 1, 2015

We report the increase in transmittance efficiency of the intermediate layer for multijunction solar cells caused by the indium–gallium–zinc–oxide (IGZO) layer used as the antireflection layer. Si substrates coated with a 200-nm-thick IGZO layer with a refractive index of 1.85 were prepared. The resistivity of the IGZO layer was increased from 0.0069 (as-deposited) to 0.032 Ω cm by heat treatment at 350 °C for 1 h to prevent free-carrier optical absorption. Samples with the Si/IGZO/adhesive/IGZO/Si structure were fabricated. The average transmissivity for wavelengths between 1200 and 1600 nm was 49%, which was close to 55% of single-crystal silicon substrates. A high effective transmittance efficiency of 89% was experimentally achieved. The numerical calculation showed an effective transmittance efficiency of 99% for 170-nm-thick antireflection layers with a resistivity of 0.6 Ω cm and a refractive index of 2.1. © 2015 The Japan Society of Applied Physics

1. Introduction

The solar cell is an attractive device, which converts sunlight energy into electrical power.^{1–5} Multijunction solar cells have been investigated as a device with a high conversion efficiency due to the effective collection of sunlight from the ultraviolet to infrared regions. Fabrication of InGaP/GaAs/Ge solar cells with a conversion efficiency of 45% by the epitaxial growth method has been reported.^{6–17} Multi junction solar cells with high conversion efficiency are attractive as a power source of space satellites as well as terrestrial power plants. Low-cost fabrication of large solar cells is important for mass production.¹⁸ We have reported the fabrication of multijunction solar cells by stacking of individual solar cells with an intermediate adhesive layer.¹⁹ The intermediate layer including indium tin oxide (ITO)²⁰ particles has successfully been used for the optical and electrical connections between the top and bottom solar cells.^{19,21} A connection resistivity of the intermediate layer lower than 1.0 Ω cm² maintains the conversion efficiency (E_{ff}) above 29.5% in the case of solar cells with an intrinsic E_{ff} of 30% and an open circuit voltage (V_{oc}) above 1.5 V.²² Moreover, we have applied the intermediate adhesive layer with dispersed ITO particles to the fabrication of multijunction compound semiconductor solar cells with a structure of InGaP/GaAs/adhesive/Ge with a E_{ff} of 15.9%, a short current density (J_{sc}) of 12.6 mA/cm², and V_{oc} of 2.13 V.^{21,22} High optical transmittance as well as electrical connection is required for high-efficiency solar cells. Reflection loss caused by the difference in the refractive index between the solar cell and intermediate adhesive layer should be reduced. In order to simultaneously achieve high optical transmittance and electrical connection with low resistivity, we have a plan of introducing two transparent and conductive layers as antireflection (AR) layers (AR layer 1 and AR layer 2) at the surfaces of top and bottom cells, as shown by schematic image in Fig. 1. When the intermediate layer is thick and the optical interference effect is sufficiently small between the surfaces, the classical optical phase matching theory gives conditions of 100% optical transmittance with zero reflection loss at wavelength (λ) as²³

$$n_{AR1} = \sqrt{n_{top}n_{intermediate}}, \quad (1)$$

$$n_{AR2} = \sqrt{n_{bottom}n_{intermediate}}, \quad (2)$$

Structure	Refractive index	Thickness
Top solar cell	n_{top}	
AR layer 1	n_{AR1}	d_{AR1}
Intermediate layer	$n_{intermediate}$	
AR layer 2	n_{AR2}	d_{AR2}
Bottom solar cell	n_{bottom}	

Fig. 1. Concept of control of reflection loss between top and bottom solar cells for multijunction solar cells.

$$d_{AR1} = \frac{(2p + 1)\lambda}{4n_{AR1}}, \quad (3)$$

$$d_{AR2} = \frac{(2q + 1)\lambda}{4n_{AR2}}, \quad (4)$$

where n_{AR1} and n_{AR2} are the refractive indexes of AR layer 1 and AR layer 2, n_{top} , $n_{intermediate}$, and n_{bottom} are the refractive indexes of the top solar cell, intermediate layer, and bottom solar cell, respectively. d_{AR1} and d_{AR2} are the thicknesses of AR layers 1 and 2, and p and q are the arbitrary numbers that express the periodicity of the optimum thickness of the AR layers, respectively. Multiple AR layers are naturally necessary for 100% optical transmittance in a wide wavelength range of the solar light. However, we pay attention to the fact that the two separate AR layers shown in Fig. 1 are still effective for practically reducing the optical reflection loss at the intermediate adhesive layer in infrared light, which is important for light absorption of the bottom cell in the multijunction solar cell.

In this paper, we discuss the reduction of reflection loss at the intermediate adhesive layer caused by the deposition of an indium–gallium–zinc–oxide (IGZO) layer, which has a low resistivity and high transmissivity.^{24–26} For basic and simple investigations, we use crystalline silicon substrates as a good sample with a high refractive index. We show the experimental results of a marked increase in transmissivity of samples in the infrared region. We also demonstrate that the control of free-carrier optical absorption of IGZO is important for achieving high transmissivity. Moreover, we analyze the experimental results and theoretically discuss the optimum conditions of thickness and refractive indexes for

high transmissivity in the infrared region using a Fresnel-type optical interference program.

2. Experimental procedure

500- μm -thick n-type Si substrates with a resistivity of 20 Ωcm were prepared. A 200-nm-thick IGZO layer with a refractive index of 1.85 was formed on the top surfaces of silicon substrates by sputtering at room temperature. We used an IGZO target with the component ratios of $\text{InGa}_{1.2}\text{ZnO}_{1.4}$. An RF power of 2 kW was applied to generate plasma of Ar gas. The deposition rate was set at 3.0 nm/s. The Si substrates coated with an IGZO layer were heated at 350 $^{\circ}\text{C}$ in air atmosphere for 1 h using a hot plate to control their resistivity.²⁷⁾ The sample was placed on the flat top table of a hot plate, which was preheated at 350 $^{\circ}\text{C}$. Then, the sample was covered with a metal cap to keep the hot air surrounding the sample during heating. A conductive transparent intermediate adhesive was formed by dispersing 20- μm -sized ITO particles in the commercial adhesive Cemedine at 6 wt%. The refractive index of Cemedine was estimated to be 1.3 from the measured transmissivity of a self-standing Cemedine film. The conductive transparent adhesive was pasted on the surface of the IGZO layer. The IGZO surface of the other sample was set on the conductive transparent adhesive layer to fabricate the Si/IGZO/adhesive/IGZO/Si structure. The Si/as-deposited IGZO/adhesive/as-deposited-IGZO/Si structure (sample I) was fabricated. Moreover, the Si/heated-IGZO/adhesive/heated-IGZO/Si structure (sample II) was also fabricated. The sample with the Si/adhesive/Si structure (control sample) was also fabricated. The intermediate conductive transparent adhesive was solidified at a pressure of 5×10^5 Pa at room temperature for 2 h. The transmissivity and reflectivity of the samples at wavelengths ranging from 500 to 2000 nm were measured by optical spectroscopy (JASCO V-700). An integrating sphere was used to calibrate the scattering caused by ITO particles.

3. Results and discussion

Figure 2(a) shows the transmissivity spectra of the single Si substrate, sample I, sample II, and control sample. The transmissivity of the single silicon substrate increased from 51 to 55% as the wavelength increased from 1150 to 2000 nm, because the refractive index of Si gradually decreases as the wavelength increases. The transmissivity of sample II was about 49% when the wavelength was in the range from 1250 to 1600 nm. Then, the transmissivity gradually decreased to 45% as the wavelength increased to 2000 nm. On the other hand, small fringes caused by optical interference of the intermediate layer were observed in the transmissivity spectrum of sample I. The transmissivity of sample I was 47% when the wavelength was 1290 nm. It decreased to 41% as the wavelength increased to 1920 nm. In the case of the control sample, the maximum transmissivity of 47% was obtained at 1590 nm and it decreased to 43% at 1970 nm. The low transmissivity of the control sample was due to the reflection loss caused by the intermediate adhesive layer.

Figure 2(b) shows the absorptivity spectra of samples I and II. Absorptivity was obtained by subtracting the transmissivity and reflectivity of a sample from 100%. Although the single Si substrate and control sample showed no absorp-

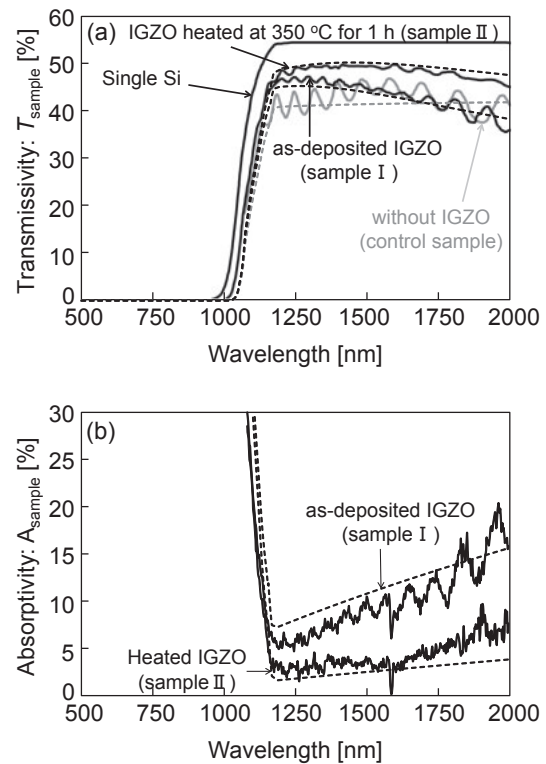


Fig. 2. Transmissivity spectra of Si/adhesive/Si, Si/as-deposited-IGZO/adhesive/as-deposited-IGZO/Si and Si/heated-IGZO/adhesive/heated-IGZO/Si samples (a). Absorptivity spectra of Si/as-deposited-IGZO/adhesive/as-deposited-IGZO, Si/heated-IGZO/adhesive/heated-IGZO/Si. The calculated transmissivity and absorptivity spectrum of each sample is shown as a dashed curve.

tivity from 1200 to 2000 nm, samples I and II showed absorptivity. The minimum absorptivity of sample I was 5.5% at 1250 nm. It increased to 15.5% as the wavelength increased to 2000 nm. On the other hand, the minimum absorptivity of sample II was 1.8% at 1250 nm. It also increased to 7.2% as the wavelength increased. The absorptivity of sample II was much lower than that of sample I. Heating markedly decreased the absorption of IGZO film.

The Fresnel-type optical calculation program, which takes into account the free-carrier absorption effect of the AR layer with low resistivity, was constructed to discuss the changes in transmissivity and absorptivity caused by the deposition of IGZO film and heating process.^{28–30)} We calculated the transmissivity and reflectivity spectra of the air/Si/AR layer/intermediate layer/AR layer/Si/air structures by taking into account the multireflection between interfaces of each layer. We assumed that the interference effect is caused by only the AR layers because the fringes of experimental transmissivity shown in Fig. 2(a) were small. The thickness and resistivity of the intermediate layer were set to be 20 μm and 500 Ωcm , which were experimentally obtained.²²⁾ AR layers 1 and 2 had a refractive index of 1.85, and a thickness of 200 nm. The resistivity of AR layers was used as a fitting parameter. The calculated transmissivity spectra were best fitted to the experimentally obtained spectra of samples I and II, and the control sample are shown as dashed curves in Fig. 2(a), and absorptivity spectra are also shown as dashed curves in Fig. 2(b). The calculated transmissivity and absorptivity spectra with the resistivity of AR layers with 0.0069 and

0.032 Ω cm were well fitted to the experimentally obtained spectra of samples I and II, respectively. The calculated transmissivity spectrum without AR layers was also well fitted to the experimentally obtained spectra of control sample. The calculated transmissivities of samples I and II decreased as the wavelength increased. The decrease in the transmissivity of sample II with 0.032 Ω cm AR layers was smaller than that of sample I with 0.0069 Ω cm AR layers. On the other hand, the calculated absorptivity spectra of samples I and II increased as the wavelength increased. Moreover, the absorptivity of sample II is much lower than that of sample I. These results are in agreement with the feature of the free-carrier absorption effect.²⁸⁾ The resistivity of the IGZO layer was increased by heating at 350 °C for 1 h. Ji et al. reported that oxygen heat treatment at 250 °C at a high pressure reduced the concentration of oxygen vacancies in IGZO.²⁷⁾ Oxygen vacancies play a role of electron donors. Therefore, the free-carrier absorption of the IGZO layer was reduced by heating, which resulted in an increase in transmissivity and a decrease in absorptivity.

To discuss the AR effect of AR layers in a wide wavelength range, we defined the effective transmittance T_{eff} as

$$T_{\text{eff}} = \int_{\lambda_1}^{\lambda_2} \frac{T_{\text{sample}}(\lambda)}{T_{\text{silicon}}(\lambda)} d\lambda, \quad (5)$$

where T_{sample} and T_{silicon} are the transmissivity of the Si/AR layer/intermediate adhesive/AR layer/Si structure and single Si substrate, respectively. The integration range from λ_1 and λ_2 are determined by the absorption edge wavelengths of the top and bottom cells, respectively. In this paper, we discuss T_{eff} in the case of stacking of Si and Ge cells as an example. λ_1 and λ_2 are 1150 and 1850 nm, respectively, because of their band gaps. The experimentally obtained T_{eff} of samples I and II and the control sample were 0.82, 0.89, and 0.79, respectively. The T_{eff} of sample II was markedly increased by the heated IGZO layers. The AR effect of the intermediate layer with heated IGZO films caused a high effective transmittance of 89% from top to bottom Si.

Figure 3 shows the calculated T_{eff} as a function of the thickness of AR layers with a refractive index of 1.85 for the AR layers with the resistivities of 0.0069, 0.032, 0.30, and 0.60 Ω cm. The calculated T_{eff} in the absence of free-carrier absorption is also shown in Fig. 3. The experimentally obtained T_{eff} values of samples I and II and the control sample are plotted as solid circles. The calculated T_{eff} periodically changed with the thickness of the AR layers. In the case of the calculated T_{eff} of 0.60 Ω cm AR layers, the first T_{eff} peak was 0.97 when the thickness of AR layer was 200 nm. The second T_{eff} peak was 0.90 at 600 nm. The calculated T_{eff} of 0.032 Ω cm AR layers also showed two peaks at 190 and 580 nm. Moreover, the calculated T_{eff} of 0.0069 Ω cm AR layers showed a low peak T_{eff} of 0.83 at 170 nm. The T_{eff} at first and second peaks decreased as resistivity was decreased by the free-carrier absorption effect. Moreover, the thickness of AR layer at the first peak of T_{eff} also decreased from 200 to 170 nm as resistivity decreased from 0.60 to 0.0069 Ω cm because of the free-carrier absorption effect. The increase in the thickness of the AR layer with a low resistivity monotonically enhances the free-carrier absorption effect, and the transmissivity of the sample decreases. In the case of the first peak of the sample with

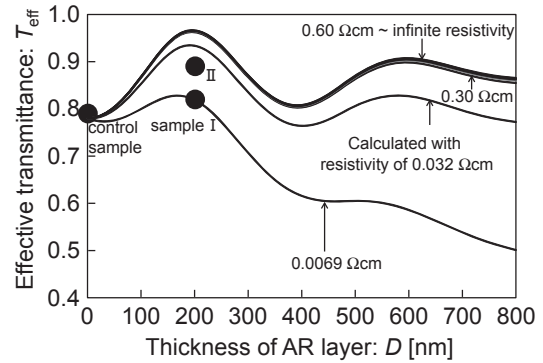


Fig. 3. Experimental and calculated effective transmittance T_{eff} as a function of D .

0.032 Ω cm AR layers, a 190-nm-thick AR layer is more advantageous than a 200-nm-thick AR layer for avoiding the free-carrier absorption effect. In the case of the calculated T_{eff} of the 0.60 Ω cm AR layers, the free-carrier absorption effect is almost negligible. Therefore, a high T_{eff} peak of 0.97 was obtained for the AR layer thickness of 200 nm.

The second T_{eff} peaks were lower than first T_{eff} peaks for all resistivities. The resonance wavelength of a sample with an AR layer with a resistivity above 0.6 Ω cm is expressed as

$$\lambda_{R(p)} = \frac{4ND}{p}, \quad (6)$$

where N and D are the refractive index and thickness of AR layers, respectively. p is an arbitrary number. When p is an odd number, $\lambda_{R(\text{odd})}$ is the wavelength under the resonant AR condition. On the other hand, when p is an even number, $\lambda_{R(\text{even})}$ is the wavelength at the original reflectivity of the substrate.

To achieve a high T_{eff} in the present wavelength range between 1150 and 1850 nm, D should be between 150 and 250 nm because $\lambda_{R(1)}$ is only included in the wavelength range between 1150 and 1850 nm. It suggests that every wavelength point is interferentially antireflective. The best D is 200 nm because $\lambda_{R(1)}$ at D of 200 nm is 1480 nm, which is almost in the central region of wavelengths between 1150 and 1850 nm. Moreover, $\lambda_{R(2)}$ at D of 200 nm is 740 nm, which is much shorter than 1150 nm. Therefore, the effect of $\lambda_{R(2)}$ on T_{eff} for the wavelength range between 1150 and 1850 nm is small. On the other hand, in the case of D between 500 and 620 nm, only $\lambda_{R(3)}$ is included in wavelength range between 1150 and 1850 nm. In this case, D of 600 nm is best because $\lambda_{R(3)}$ at D of 600 nm is 1480 nm, which is almost in the central region of the wavelengths between 1150 and 1850 nm. However, $\lambda_{R(4)}$ at D of 600 nm is 1110 nm, which is close to wavelength of 1150 nm and $\lambda_{R(3)}$ of 1480 nm. In this case, interaction between $\lambda_{R(3)}$ and $\lambda_{R(4)}$ decreases T_{eff} at D of 600 nm. Therefore, T_{eff} of the first peak at 200 nm was higher than that of the second peak at 600 nm. These results suggest that thin AR layers are suitable for achieving a high T_{eff} .

The calculated T_{eff} without AR layers ($D = 0$) was 0.78. This result was in good agreement with the experimental T_{eff} of the control sample. The T_{eff} of sample I was well fitted to the calculated T_{eff} curve with the AR layer with the resistivity of 0.0069 Ω cm and thickness of 200 nm. The experimental

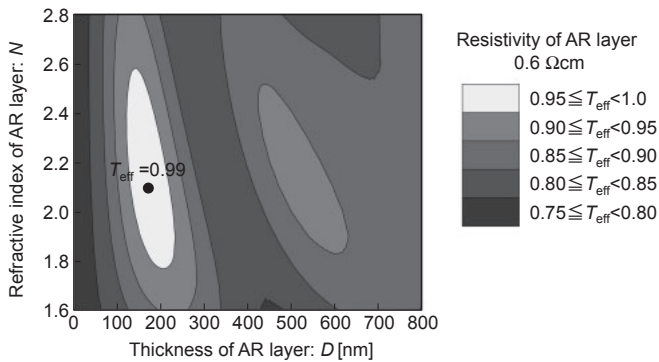


Fig. 4. Distribution of T_{eff} obtained at N values from 1.6 to 2.8 and D values from 0 to 800 nm.

T_{eff} of the sample II was also close to the calculated T_{eff} with the AR layer with the resistivity of $0.032 \Omega \text{ cm}$ and thickness of 200 nm. Good AR effect in a wide range of wavelengths between 1150 to 1850 nm was obtained for the sample II.

Sample II showed a high T_{eff} of 0.89. However, the numerical calculation of T_{eff} , as shown in Fig. 3, suggests that the free-carrier absorption of sample II is not negligible and it decreased T_{eff} . Therefore, AR layers with resistivities higher than $0.032 \Omega \text{ cm}$ are required for achieving high T_{eff} . On the other hand, the high resistivity of AR layers causes the increase in the connection resistivity of intermediate layers. From the results of our investigation, 800-nm-thick AR layers with the resistivities between 0.6 and $600 \Omega \text{ cm}$ simultaneously satisfy the condition of negligibly small free-carrier absorption and connection resistivities lower than $1.0 \Omega \text{ cm}^2$. Then we calculated T_{eff} of samples with $0.60 \Omega \text{ cm}$ -AR layers at various values of N (1.6 to 2.8) and D (0 to 800 nm) to determine the optimum conditions of materials and thickness of AR layers for achieving a high T_{eff} .

Figure 4 shows the distribution of T_{eff} calculated at various N and D values. T_{eff} periodically changed as D changed for each N . The peaks of T_{eff} were observed at D values of approximately 200 and 500 nm. The first peak at small D values was higher than second peak at large D values. The low T_{eff} of the second peak was due to the low transmissivity between 1150 to 1850 nm caused by the interaction between $\lambda_{R(\text{odd})}$ and $\lambda_{R(\text{even})}$. The maximum T_{eff} of 0.99 was obtained when N and D were 2.1 and 170 nm, respectively, as indicated by a solid circle in Fig. 4. The N of 2.1 is close to the optimum refractive index of the AR layer for a single-wavelength light expressed by Eqs. (1) and (2). The condition of refractive index for a high transmissivity between 1150 to 1850 nm was satisfied. Moreover, the resonance wavelength obtained using Eq. (6) with N and D of 2.1 and 170 nm, respectively, was 1428 nm, which was close to the central region of wavelengths between 1150 and 1850 nm. 170-nm-thick AR layers are sufficiently thin to maintain the high transmissivity of samples at wavelengths from 1150 to 1850 nm. Moreover, T_{eff} above 0.95 was obtained in an oval-shaped area with N values from 1.8 to 2.6 and D values from 125 to 220 nm. These results indicate that there are many choices of materials for the AR layer of multijunction solar cells. In this study, we used IGZO as the AR layer because its resistivity can be changed by post-annealing. However, it is known that ZnO has a refractive index of 2.0.³¹ Carcia

et al. reported that the resistivity of the ZnO films was controlled by varying the partial pressure of oxygen gas during sputtering.³² Therefore, we believe that ZnO films, as well as IGZO, with a high concentration of oxygen are a promising candidate as the AR layer for multijunction solar cells. Moreover, we can estimate the reflection loss of stacked samples with other AR layers and cells. We believe that the selection of the optimum $n_{\text{AR}1}$, $n_{\text{AR}2}$, $d_{\text{AR}1}$, and $d_{\text{AR}2}$ of two AR layers gives a high T_{eff} for stacking of various types of solar cell.

4. Conclusions

We investigated the increase in the transmittance of the intermediate adhesive layer for multijunction solar cells. The Si/as-deposited IGZO/adhesive/as-deposited IGZO/Si sample (sample I) was fabricated. Moreover, Si/heated-IGZO/adhesive/heated-IGZO/Si (sample II) was also fabricated. In the case of sample II, its transmissivity was about 49% when the wavelengths ranged from 1250 to 1600 nm. The transmissivity of sample II was much higher than that of the Si/adhesive/Si (control sample) sample. The absorptivity of sample I was 5.5% at 1250 nm. It increased to 15.5% as the wavelength increased to 2000 nm. On the other hand, the absorptivity of sample II was 1.8% at 1250 nm. According to the numerical calculation of transmissivity spectra using Fresnel-type optical calculation program, the resistivity of the IGZO film was increased from 0.0069 to $0.032 \Omega \text{ cm}$ by heat treatment at 350°C for 1 h. The decrease in the concentration of oxygen vacancy in the IGZO film by heat treatment resulted in the increase in transmissivity and decrease in absorptivity. We also showed the effective transmittance of T_{eff} of the samples. Although the T_{eff} of the control sample was 0.79, samples I and II showed high T_{eff} of 0.82 and 0.89, respectively. The results indicate that our current IGZO film may be applied to mechanical stack multijunction solar cells. According to the calculation of the T_{eff} of the Si/ $0.6 \Omega \text{ cm}$ -IGZO/adhesive/ $0.6 \Omega \text{ cm}$ -IGZO/Si structure, a high T_{eff} of 0.99 was obtained when N and D were 2.1 and 170 nm, respectively. We believe that there is possibility of effective reduction of reflection loss for multijunction solar cells by selection of the optimum N and D of AR layers.

Acknowledgements

This work was partly supported by the New Energy and Industrial Technology Development Organization (NEDO), Grant-in-Aid for Scientific Research C (No. 25420282) from the Ministry of Education, Culture, Sports, Science and Technology of Japan, The Naito Science and Engineering Foundation, and Sameken Co., Ltd.

- 1) M. Tanaka, M. Taguchi, T. Matsuyama, T. Sawada, S. Tsuda, S. Nakano, H. Hanafusa, and Y. Kuwano, *Jpn. J. Appl. Phys.* **31**, 3518 (1992).
- 2) J. Zhao, A. Wang, M. A. Green, and F. Ferrazza, *Appl. Phys. Lett.* **73**, 1991 (1998).
- 3) O. Schultze, S. W. Glunz, and G. P. Willeke, *Prog. Photovoltaics* **12**, 553 (2004).
- 4) A. V. Shah, H. Schade, M. Vanecek, J. Meier, E. Vallat-Sauvain, N. Wyrsh, U. Kroll, C. Droz, and J. Bailat, *Prog. Photovoltaics* **12**, 113 (2004).
- 5) S. Chhajed, M. F. Schubert, J. K. Kim, and E. F. Schubert, *Appl. Phys. Lett.* **93**, 251108 (2008).
- 6) H. Sugiura, C. Amano, A. Yamamoto, and M. Yamaguchi, *Jpn. J. Appl.*

- Phys. **27**, 269 (1988).
- 7) J. M. Olson, S. R. Kurtz, A. E. Kibbler, and P. Faine, *Appl. Phys. Lett.* **56**, 623 (1990).
 - 8) T. Takamoto, E. Ikeda, H. Kurita, M. Ohmori, M. Yamaguchi, and M. J. Yang, *Jpn. J. Appl. Phys.* **36**, 6215 (1997).
 - 9) M. Yamaguchi, *Sol. Energy Mater. Sol. Cells* **75**, 261 (2003).
 - 10) M. Yamaguchi, T. Takamoto, K. Araki, and N. Ekins Daukes, *Sol. Energy* **79**, 78 (2005).
 - 11) M. Yamaguchi, T. Takamoto, and K. Araki, *Sol. Energy Mater. Sol. Cells* **90**, 3068 (2006).
 - 12) M. Yamaguchi, K. Nishimura, T. Sasaki, H. Suzuki, K. Arafune, N. Kojima, Y. Oshita, Y. Okada, A. Yamamoto, T. Takamoto, and K. Araki, *Sol. Energy* **82**, 173 (2008).
 - 13) E. A. Katz, J. M. Gordon, and D. Feuermann, *Prog. Photovoltaics* **14**, 297 (2006).
 - 14) F. Meillaud, A. Shah, C. Droz, E. Vallat-Sauvain, and C. Miazza, *Sol. Energy Mater. Sol. Cells* **90**, 2952 (2006).
 - 15) R. R. King, D. C. Law, K. M. Edmondson, C. M. Fetzer, G. S. Kinsey, H. Yoon, R. A. Sherif, and N. H. Karam, *Appl. Phys. Lett.* **90**, 183516 (2007).
 - 16) D. J. Friedman, *Curr. Opin. Solid State Mater. Sci.* **14**, 131 (2010).
 - 17) A. Hadipour, B. D. Boer, and P. W. M. Blom, *Adv. Funct. Mater.* **18**, 169 (2008).
 - 18) T. Saga, *NPG Asia Mater.* **2**, 96 (2010).
 - 19) T. Sameshima, J. Takenezawa, M. Hasumi, T. Koida, T. Kaneko, M. Karasawa, and M. Kondo, *Jpn. J. Appl. Phys.* **50**, 052301 (2011).
 - 20) T. Karasawa and Y. Miyata, *Thin Solid Films* **223**, 135 (1993).
 - 21) S. Yoshidomi, M. Hasumi, T. Sameshima, K. Makita, K. Matsubara, and M. Kondo, Proc. 6th Thin Film Materials and Devices Meet., 2013, 130222027-1.
 - 22) S. Yoshidomi, M. Hasumi, and T. Sameshima, *Appl. Phys. A* **116**, 2113 (2014).
 - 23) S. Walheim, E. Schäffer, J. Mlynek, and U. Steiner, *Science* **283**, 520 (1999).
 - 24) T. Kamiya, K. Nomura, and H. Hosono, *J. Disp. Technol.* **5**, 273 (2009).
 - 25) J. H. Na, M. Kitamura, and Y. Arakawa, *Appl. Phys. Lett.* **93**, 063501 (2008).
 - 26) K. Nomura, H. Ohta, A. Takagi, T. Kamiya, M. Hirano, and H. Hosono, *Nature* **432**, 488 (2004).
 - 27) K. H. Ji, J. Kim, H. Y. Jung, S. Y. Park, R. Choi, U. K. Kim, C. S. Hwang, D. Lee, H. Hwang, and J. K. Jeong, *Appl. Phys. Lett.* **98**, 103509 (2011).
 - 28) K. Ukawa, Y. Kanda, T. Sameshima, N. Sano, M. Naito, and N. Hamamoto, *Jpn. J. Appl. Phys.* **49**, 076503 (2010).
 - 29) T. Sameshima, K. Saito, M. Sato, A. Tajima, and N. Takashima, *Jpn. J. Appl. Phys.* **36**, L1360 (1997).
 - 30) T. Sameshima, K. Saito, N. Aoyama, M. Tanda, M. Kondo, A. Matsuda, and S. Higashi, *Sol. Energy Mater. Sol. Cells* **66**, 389 (2001).
 - 31) R. G. Heideman, P. V. Lambeck, and J. G. E. Gardeniers, *Opt. Mater.* **4**, 741 (1995).
 - 32) P. F. Carcia, R. S. McLean, M. H. Reilly, and G. Nunes, *Appl. Phys. Lett.* **82**, 1117 (2003).